Electronic Supplementary Material (ESI) for ChemComm.
This journal is © The Royal Society of Chemistry 2014

Supporting information for

Towards enantioselective adsorption in surface-confined nanoporous systems

Elke Ghijsens,[a] Hai Cao,[a] Aya Noguchi,[b] Oleksandr Ivasenko,[a] Yuan Fang,[a] Kazukuni Tahara,[b] Yoshito Tobe[b] and Steven De Feyter[a]

[a] KU Leuven, Celestijnenlaan 200F, 3001 Heverlee, Belgium.

[b] Division of Frontier Materials Science, Graduate School of Engineering Science, Osaka University, Toyonaka, Osaka 560-8531, Japan.

Contents:

1. Experimental Section

Synthesis of the target compounds, achiral and chiral DBAs: DBA-OC12, DBA-OC13, cDBA-OC12(*S*) and cDBA-OC13(*R*) were synthesised according to a previously reported method. (*J. Am. Chem. Soc.*, 2006, **128**, 16613–16625.; *Nat. Chem.*, 2011, **3**, 714–719.). The synthesis of cDBA-OC12(*R*) is reported in **Section 9**.

Solution preparation: 1-octanoic acid (Sigma-Aldrich, 99%, used as received) and 1-phenyloctane (Sigma-Aldrich, 99%, used as received) were used as solvents to dissolve the DBA molecules. The concentrations used in each experiment are specified in the following captions.

STM measurements: All STM experiments were performed at room temperature (20–23 ^{o}C) using a PicoSPM (Molecular imaging, now Agilent) machine operating in constant–current mode with the tip immersed in the supernatant liquid. STM tips were prepared by mechanical cutting from Pt/Ir wire (80%/20%, diameter 0.2 mm). Prior to imaging, a drop of the solution was applied onto a freshly cleaved surface of highly oriented pyrolytic graphite (HOPG, grade ZYB, Advanced Ceramics Inc., Cleveland, USA). For analysis purposes, recording of a monolayer image on HOPG was followed by consecutive imaging the graphite substrate underneath. This was done under the same experimental conditions but by lowering the substrate bias (typically V_{bias} = 1 mV) and increasing the tunnelling current (typical I_{set} = 800 pA). From the atomically resolved STM image of HOPG one can easily obtain the graphite symmetry axes. The images were corrected for drift via Scanning Probe Image Processor (SPIP) software (Image Metrology ApS), using the graphite lattice, allowing a more accurate unit cell

determination. From the corrected graphite images three main symmetry axes and also three reference axes (normal to main symmetry axes) can be determined. The images are low-pass filtered. The imaging parameters are indicated in the figure caption: tunneling current (I_{set}), and sample bias (V_{bias}).

Data processing: Analysis was performed by grouping images taken after a specific drop of the solution was applied to the surface. In that way approximately 10 images were grouped into what is called a session. A new session was established only after applying a new drop of the solution onto a freshly cleaved HOPG surface. Within the same scan area maximum 4 images were recorded (each at every corner). Next the images were plane corrected by using SPIP software (Image Metrology A/S).

To analyse the handedness of the dimer types and hexagons on the surface, high resolution images were recorded. Chirality can be resolved clearly when the image size is around 70×70 nm^2. The honeycomb surface coverage was calculated based on 3 sessions (j) of 10 large scale images. Because the complete dataset of images is not all of a same size a weighted mean $\overline{P}$ and weighted standard deviation σ were calculated according to the following equations respectively.

After plane correcting the images, the surface area occupied by the porous structure (A_s) was measured. Then the number of CW ($N_{CW,ij}$), non-*C*6 ($N_{non,ij}$), and CCW ($N_{CCW,ij}$) hexagons in every image (*i*) and in every session (*j*) were counted. The error bar was calculated as a weighted standard deviation σ as presented in the following equations. In this way the error bar represents the variation between the different

sessions and not the error on the correctness of assigning a CW, non-*C*6 or CCW hexagon type.

$$\bar{P} = \frac{\sum_{j=1}^{3} A_{s,j} P_{CW,j}}{\sum_{j=1}^{3} \sum_{i=1}^{n} A_{s,ij}}$$

$$\text{with } P_{CW,j} = \frac{\sum_{j}^{j} \sum_{i=1}^{n} N_{CW,ij}}{\sum_{j}^{j} \sum_{i=1}^{n} N_{CW,ij} + \sum_{j}^{j} \sum_{i=1}^{n} N_{non,ij} + \sum_{j}^{j} \sum_{i=1}^{n} N_{CCW,ij}}$$

$$\sigma = \sqrt{\frac{\sum_{j=1}^{3} A_{s,j} \left(P_{CW,j} - \bar{P}\right)^2}{\sum_{j=1}^{3} \sum_{i=1}^{n} A_{s,ij}}}$$

The guest molecules can only be well visualized at a specific state of the tip, and only high resolution images were selected for the statistics of guest adsorption, preferably images contain both CW and CCW domains. The number of nanowells being analysed are specified in each table. The error bars were calculated using the above mentioned method.

2. Induced chirality: sergeants and soldiers principle.

Table S1 The mixing ratio dependent changes of CW and CCW honeycomb structures for mixtures of achiral DBA and corresponding chiral analogue.

Identity of cDBA	10 mol% cDBA[a]			30 mol% cDBA[a]			30 mol% cDBA[b]			50 mol% cDBA[a]			90 mol% cDBA[a]		
	CW (%)	non-C6 (%)	CCW (%)	CW (%)	non-C6 (%)	CCW (%)	CW (%)	non-C6 (%)	CCW (%)	CW (%)	non-C6 (%)	CCW (%)	CW (%)	non-C6 (%)	CCW (%)
cDBA-OC12(*S*)	82±4	0.8±0.1	17±4	95±3	0.8±0.4	4±3	-	-	-	96±3	0.8±0.5	3±3	100±1	0.2±0.2	0±0
cDBA-OC12(*R*)	22±4	0.8±0.2	77±4	9±1	0±0	91±1	-	-	-	4±4	0.4±0.2	95±4	0±0	0±0	100±1
cDBA-OC13(*R*)	7±1	3.9±2.0	89±3	8±2	1.0±0.7	91±2	9±4	1.6±0.1	90±4	0±0	0.6±0.6	99±1	0±0	0±0	100±0

a: premixed samples in 1-phenyloctane, with a total concentration of 2.5×10^{-6} mol/L.
b: premixed samples in 1-octanoic acid, with a total concentration of 1×10^{-6} mol/L.

3. Supplementary STM images for Fig. 2

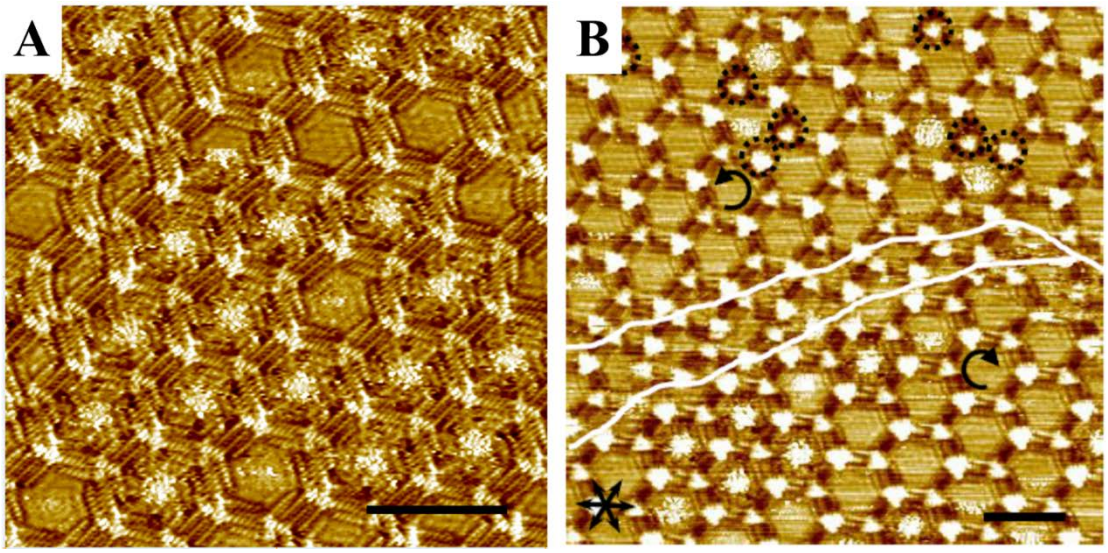

Fig. S1 Supplementary STM images of premixed solutions containing (A) 30 mol% cDBA-OC12(*S*)/70 mol% DBA-OC12 (I_{set} = 200 pA and V_{bias} = –250 mV) and (B) 30 mol% cDBA-OC12(*R*)/70 mol% DBA-OC12 (I_{set} = 200 pA and V_{bias} = –200 mV). The white lines marks the boundary between a CCW domain and CW domain. The black arrows indicate the major symmetry axes of the HOPG surface underneath. The scale bars measure 5 nm. The black dots indicate cDBA-OC12(*R*) sergeant molecules.

4. Guest adsorption in monolayer originally formed by pure achiral or chiral DBA

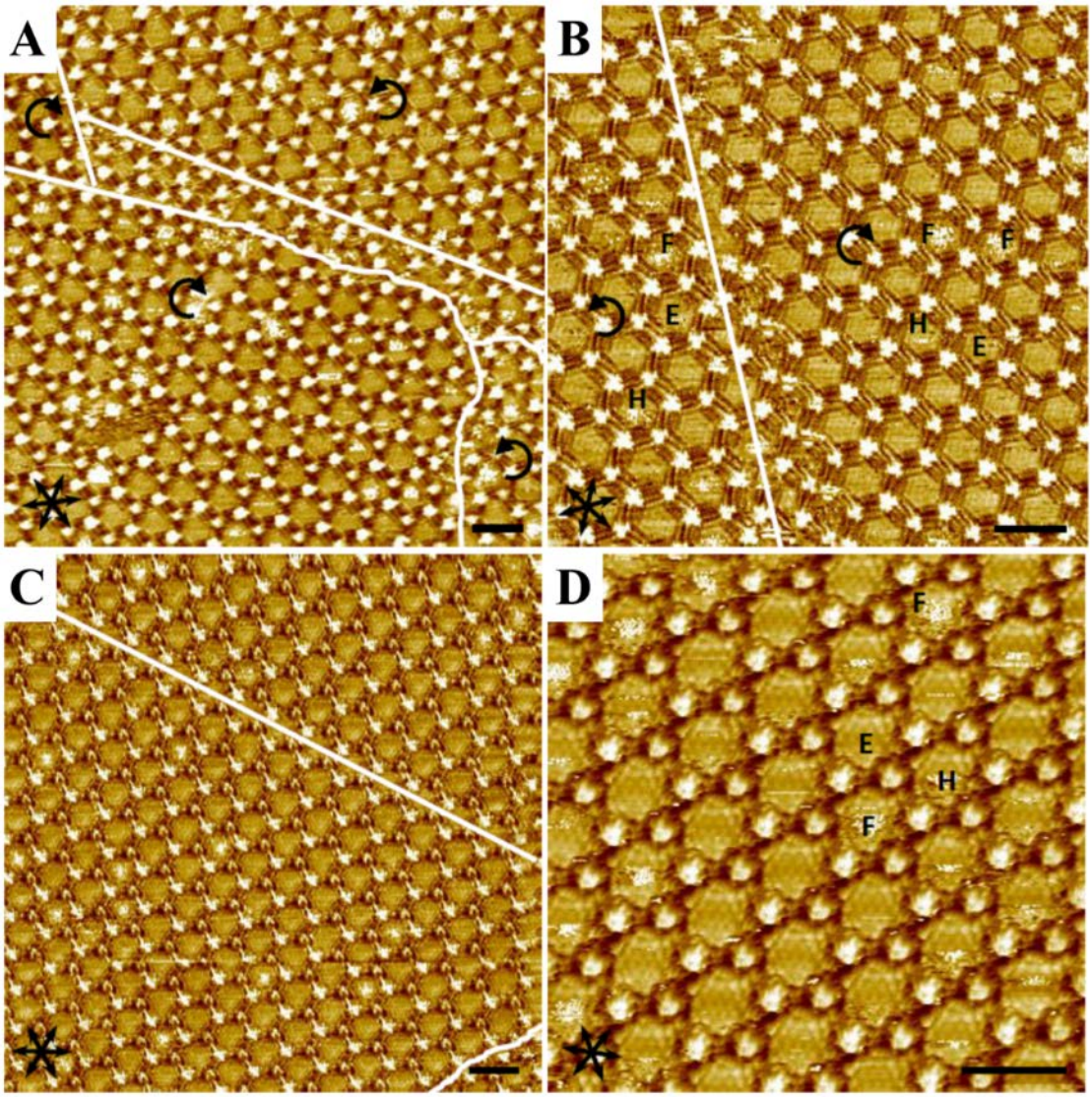

Fig. S2 (A, B) STM-images (I_{set} = 200 pA and V_{bias} = –200 mV) of the self-assembled structure deposited from a solution of pure DBA-OC12 dissolved in phenyloctane with concentration 2.5 × 10^{-6} M. and (C, D) STM-images of the self-assembled structure deposited from a solution of pure cDBA-OC12(*S*) with concentration 2.5 × 10^{-6} M. (C) Large scale images showing small number of occupied pores (I_{set} = 195 pA and V_{bias} = –220 mV). (D) High resolution image (I_{set} = 265 pA and V_{bias} = –200 mV). Some pores in the high resolution images (B, D) were indicated as fuzzy (F), half-fuzzy (H) and empty (E). The HOPG main symmetry directions are represented by the black arrow in the left corner. The scale bars are 5 nm.

Table S2 Characteristics of guest adsorption in the adlayer of pure DBA-OC12 and pure cDBA-OC12(*S*). 'Total pores' specifies the complete dataset used to calculate the occupation degree.

Pure DBA (cDBA) samples	DBA-OC12 (2.5×10^{-6} M)			cDBA-OC12(*S*) (2.5×10^{-6} M)		
	CCW (%)	non-C6 (%)	CW (%)	CCW (%)	non-C6 (%)	CW (%)
Total pores	562	3	580	0	9	1777
Incorporated	0±0	0±0	0±0	0	0±0	0±0
Fuzzy	14±3	0±0	16±4	0	0±0	4±3
Half fuzzy	10±2	0±0	9±4	0	0±0	6±3
Empty	76±4	100±/	74±5	0	100±/	90±4

5. Dynamics of enantioselective adsorption

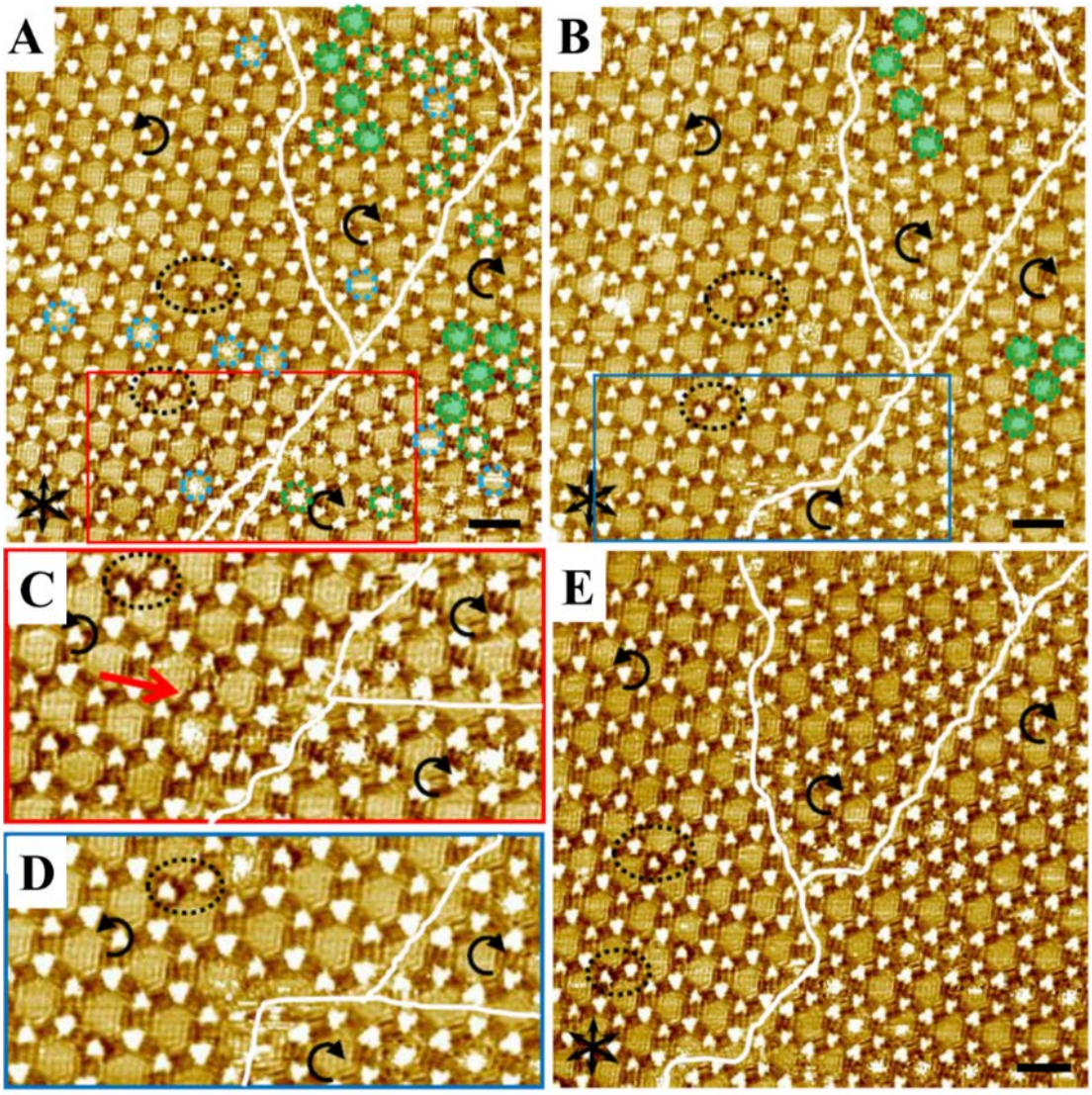

Fig. S3 Sequential STM-images (I_{set} = 200 pA and V_{bias} = –200 mV) of a same area to view the dynamics of guest molecules and the chiral molecules as co-adsorbed in the adlayer network. cDBA-OC12(*R*) was deposited 30 min after achiral DBA-OC12. The images at relative time scales of (A) 0 min, (B) 2 min (consecutive right after image a) and (E) 7 min show no movement of the chiral DBA molecules (identified by black contour, marked with black dots) as part of the host network. (A, B) Guest molecules highlighted by green circles are defined as *incorporated*. The guests surrounded with filled circles did not move between consecutive images. Guest molecules highlighted by the blue circles appeared as *fuzzy* and *half-fuzzy*. (C, D) Enlarged areas of images A and B respectively. A chiral DBA molecule that is part of the host network nearby a domain border (pinpointed by the red arrow) gets easily desorbed. The HOPG main symmetry directions are represented by the black arrow in the left corner. The scale bars are 5 nm.

Table S3 Characteristics of guest adsorption in the adlayer of premixed solution of 30 mol% cDBA-OC12(*S/R*) and 70 mol%DBA-OC12 by taking into account time frame of the STM-measurements. 'Total pores' specifies the complete dataset used to calculate the occupation degree.

Premixed samples	30 mol% cDBA-OC12(*S*) (30 min)			30 mol% cDBA-OC12(*R*) (2 h)		
	CCW (%)	non-C6 (%)	CW (%)	CCW (%)	non-C6 (%)	CW (%)
Total pores	356	5	1580	1272	13	116
Incorporated	12±8	0±0	0±0	0±0	0±0	14±1
Fuzzy	6±6	0±0	9±5	8±1	0±0	6±2
Half fuzzy	10±7	4±/	11±6	13±2	23±0	26±3
Empty	73±8	100±/	79±4	78±5	77±/	54±13

6. Molecular modelling

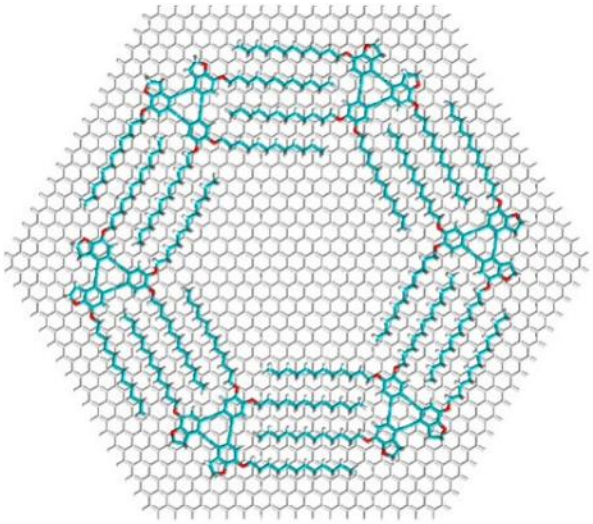

Fig. S4 Optimized hexamers of modified DBA-OC12 on a frozen graphene flake.

All molecular mechanics calculations were performed with MM+ force field as implemented in HyperChem Prof. 7.52 (HyperChem (TM) Professional 7.52, H., Inc., 1115 NW 4th Street, Gainesville, Florida 32601, USA, 2002). Geometries were optimized to rms deviation of the energy gradient smaller than 0.01 kcal/(mol·Å). Using protocol developed and tested previously (*ACS Nano*. 2013, **7**, 8031–8042), we have designed and optimized hexamers of modified DBA-OC12 on a frozen graphene flake (**Fig. S4**). Here alkoxy chains not participating in the interactions were truncated. This allowed exclusion of undesirable fluctuations in adsorption energies due to flexibility of these chains, while still maintaining similar electronic structure and parallel orientation of the DBA core.

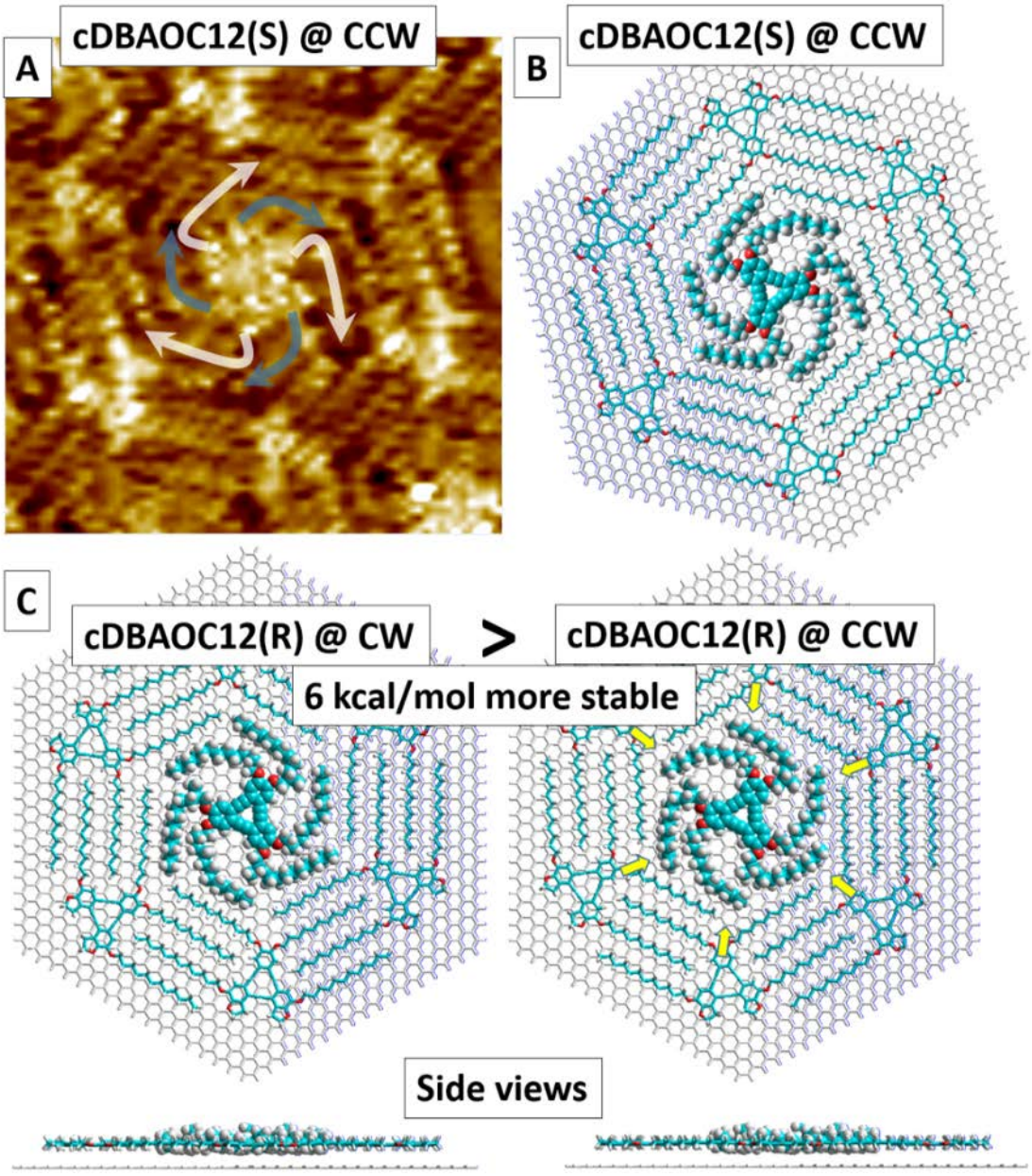

Fig. S5 Modelling of completely confined ('incorporated') cDBA-OC12(*S*/*R*) guest molecules inside DBA-OC12 networks. A) STM image of an incorporated guest (Obtained from premixed solution with 30 mol% cDBA-OC12(*S*) and 70 mol% DBA-OC12) suggesting tentative bending (marked with semitransparent white and grey arrows) of its alkyl chains. This STM image, free from the arrows, can be seen in Fig. 2B of the main manuscript. B) MM-optimized molecular model of cDBA-OC12(*S*) inside DBA-OC12 hexamer. C) Optimized molecular geometry and energy difference of two host-guest complexes. Here, yellow arrows point to the regions where the alkyl chains of the guest (cDBA-OC12(*R*)) do not have efficient van der Waals contacts with the alkyl chains of the CCW pore. Corresponding contacts are present in the case of cDBA-OC12(*R*)@CW host-guest complex and constitute the primary reason for its higher stability compared to cDBA-OC12(*R*)@CCW complex.

To model guest molecules completely confined (incorporated) within DBA pores we have tested several conformations and found that the lowest energy geometry features bent alkyl chains (**Fig. S5A**) with stereogenic methyl groups pointing up from the substrate to avoid the steric repulsion with substrate (**Fig. S5B**). Optimization of the chiral guests inside CW and CCW pores show some enantioselectivity. For example, cDBA-OC12(*R*) prefers to adsorb within CW pores of DBAOC12 net (**Fig. S5C**).

7. Guest adsorption in premixed samples with 10 mol% chiral DBA

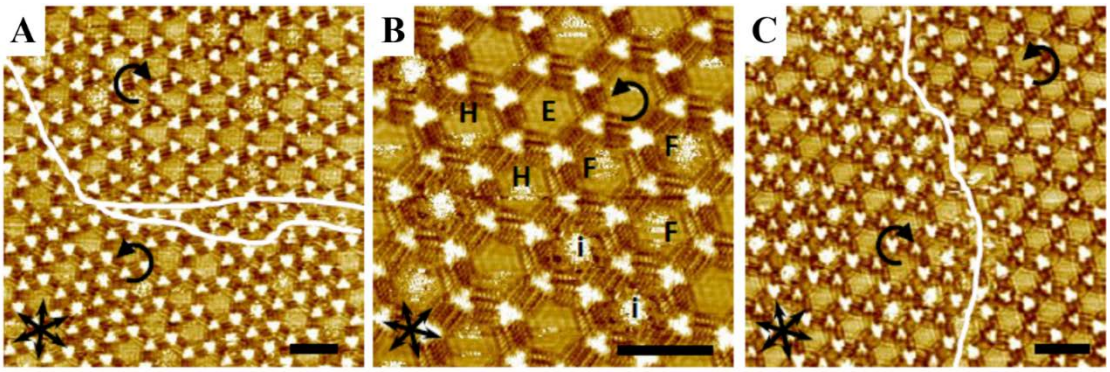

Fig. S6 STM-images of premixed solutions containing 10 mol% chiral DBA. (A) Large scale image (I_{set} = 180 pA and V_{bias} = –200 mV) of the adlayer adsorbed from a solution containing cDBA-OC12(*S*). (B) High resolution image (I_{set} = 200 pA and V_{bias} = –250 mV) of a CCW domain. Some occupied pores are assigned as half-fuzzy (H), fuzzy (F) and incorporated (I). The empty pores are pinpointed with the letter E. (C) Large scale image (I_{set} = 200 pA and V_{bias} = –200 mV) of the adlayer adsorbed from a solution containing cDBA-OC12(*R*). The HOPG main symmetry directions are represented by the black arrow in the left corner. The scale bars are 5 nm.

Table S4 Characteristics of guest adsorption in the adlayer of 1:9 (10 mol% cDBA) premixed solution of cDBA-OC12(*S/R*) and DBA-OC12. 'Total pores' specifies the complete dataset used to calculate the occupation degree.

Premixed samples	10 mol% cDBA-OC12(*S*)			10 mol% cDBA-OC12(*R*)		
	CCW (%)	non-C6 (%)	CW (%)	CCW (%)	non-C6 (%)	CW (%)
Total pores	591	28	3075	2413	16	945
Incorporated	33±1	0±0	1±0	3±1	0±0	10±2
Fuzzy	6±3	0±0	15±3	9±2	0±0	17±7
Half fuzzy	4±2	4±/	5±2	8±1	0±0	8±1
Empty	57±3	96±/	79±1	81±2	100±/	65±7

8. Porous networks formed by DBA-OC13 and cDBA-OC13(*R*)

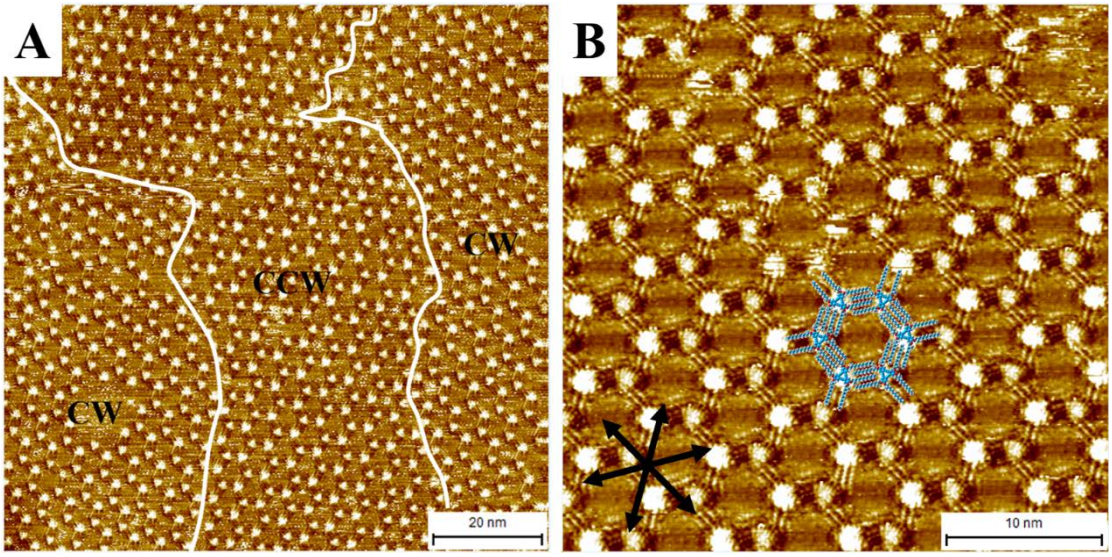

Fig. S7 STM images of (A) DBA-OC13 (1×10^{-6} M, I_{set} = 280 pA and V_{bias} = –230 mV) and (B) cDBA-OC13(*R*) (1×10^{-6} M, I_{set} = 280 pA and V_{bias} = –230 mV) at the 1-octanoic acid/HOPG interfaces. For chiral DBA, only CCW nanowells were obtained. The white lines marks the boundary between a CCW domain and CW domain. The black arrows indicate the major symmetry axes of the HOPG surface underneath.

9. Synthesis of cDBA-OC12(*R*).

General. All manipulations were performed in an inert gas (nitrogen or argon) atmosphere. All solvents were distilled before use. All commercially available reagents were used as received.

^{1}H (400 MHz) and ^{13}C (100 MHz) NMR spectra were measured on a Brucker UltraShield Plus 400 spectrometer. When chloroform-*d* was used as solvent, the spectra were referenced to residual solvent proton signals in the ^{1}H NMR spectra (7.26 ppm) and to the solvent carbons in the ^{13}C NMR spectra (77.0 ppm). Other spectra were recorded by the use of the following instruments: IR spectra, JACSCO FT/IR-410; mass spectra, JEOL JMS-700 for EI or FAB ionization mode.

Scheme S1 Synthesis of cDBA-OC12(*R*).

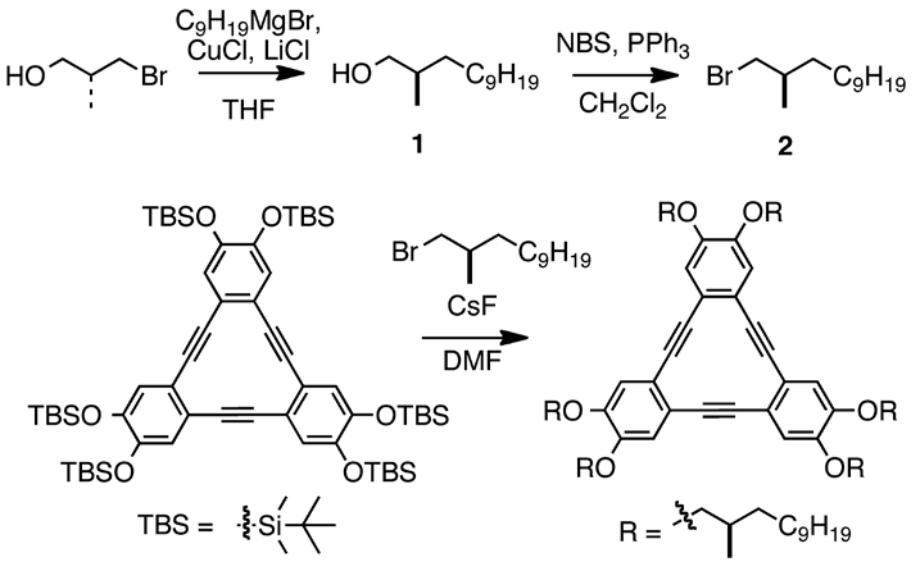

Synthesis of (*R*)-2-Methyldodecan-1-ol (1). To a suspension of magnesium (957 mg, 39.4 mmol) in THF (12.0 mL), 1-bromononane (4.08 g, 19.7 mmol) was added dropwise via a syringe. After stirring for 2 h at room temperature, prepared Grignard reagent was transferred to another reaction vessel via a cannula. The reaction vessel

was cooled in an ice bath. A solution of $CuCl_2$ (334 mg, 2.49 mmol) and LiCl (217 mg, 5.12 mmol) in THF (5.0 mL) was added to the mixture. Then, a solution of (*S*)-3-bromo-2-methyl-1-propanol (504 mg, 3.29 mmol) in THF (1.1 mL) was added to the mixture. After stirring at 50 °C for 19 h, the reaction was quenched by the addition of saturated solution of NH_4Cl aq. (2 mL) and water. The products were extracted with ether, and the extract was washed with an aqueous solution of NH_3 (ca. 5%) and brine. The extract was dried over $MgSO_4$. After removal of the solvents under vacuum, the crude mixture was subjected to a silica gel column (hexane/AcOEt = 8/1) to give **1** (444 mg, 67%) as a colorless oil. ^{1}H NMR (400 MHz, $CDCl_3$, 30 °C) δ 3.54–3.49 (m, 1H), 3.46–3.37 (m, 1H), 1.67–1.56 (m, 1H), 1.46–1.01 (m, 18H), 0.97–0.77 (m, 6H); ^{13}C NMR (100 MHz, $CDCl_3$, 30 °C) δ 68.4, 35.8, 33.2, 31.9, 29.9, 29.7, 29.6, 29.3, 27.0, 22.7, 16.6, 14.1; IR (neat) 3334, 2956, 2925, 2854, 1466, 1378, 1041, 721 cm^{-1}; MS (EI): *m/z* = 182 ($[M-H_2O]^+$).

Synthesis of (*R*)-1-Bromo-2-methyldodecane (2). To a solution of **2** (40.9 mg, 204 μmol) in CH_2Cl_2 (0.6 mL) at 0 °C, PPh_3 (80.8 mg, 308 μmol) and *N*-bromosuccinimide (NBS, 55.3 mg, 311 μmol) were added. After stirring at room temperature for 30 min, the solvent was removed under vacuum. The products were separated with a silica gel column (hexane) to afford **2** (48.6 mg, 91%) as a colorless oil. ^{1}H NMR (400 MHz, $CDCl_3$, 30 °C) δ 3.40 (dd, *J* = 9.6, 5.0 Hz, 1H), 3.32 (dd, *J* = 9.6, 6.0 Hz, 1H), 1.87–1.70 (m, 1H), 1.50–1.11 (m, 18H), 1.01 (d, *J* = 6.4 Hz, 3H), 0.88 (t, *J* = 6.8 Hz, 3H); ^{13}C NMR (100 MHz, $CDCl_3$, 30 °C) δ 41.5, 35.2, 34.9, 31.9, 29.7, 29.61, 29.58, 29.3,

26.9, 22.7, 18.8, 14.1; IR (neat) 2957, 2925, 2854, 1464, 1378, 1229, 939, 820, 721, 653, 622 cm^{-1}; HRMS (EI): *m/z* calcd for $C_{13}H_{27}{}^{81}Br$ (M^+) 264.1276, Found: 264.1266.

Synthesis of cDBA-OC12(*R*). *Tert*-Butyldimethylsilyl protected hexahydroxy DBA (21.5 mg, 19.9 μmol) was dissolved in DMF (0.5 mL). To the solution, CsF (46.3 mg, 305 μmol) and a solution of **2** (91.7 mg, 348 μmol) in DMF (1.5 mL) were added at room temperature. After stirring at 80 °C for 3 h, the solvent was removed under vacuum. The residue was subjected to silica gel column chromatography (hexane/CH_2Cl_2 = from 60/1 to 6/1) to give **cDBA-OC12(*R*)** (14.1 mg, 48%) as a yellow oil. ^{1}H NMR (400 MHz, $CDCl_3$, 30 °C) δ 6.70 (s, 1H), 3.79 (dd, *J* = 8.8, 6.0 Hz, 6H), 3.72 (dd, *J* =8.8, 6.8 Hz, 6H), 2.10–1.87 (m, 6H), 1.52–1.16 (m, 108H), 1.02 (d, *J* = 6.8 Hz, 18H), 0.88 (t, *J* = 6.8 Hz, 18H); ^{13}C NMR (100 MHz, $CDCl_3$, 30 °C) δ 149.4, 119.7, 115.7, 91.9, 74.0, 33.5, 33.2, 31.9, 29.9, 29.71, 29.65, 29.4, 27.0, 22.7, 17.0, 14.1; IR (KBr) 3082, 2953, 2923, 2852, 2206, 1693, 1593, 1550, 1529, 1510, 1467, 1414, 1377, 1354, 1259, 1228, 1070, 1014, 926, 887, 855, 799, 723 cm^{-1}; HRMS (FAB): *m/z* calcd for $C_{102}H_{168}O_6$ (M^+) 1489.2841, Found: 1489.2848.